LA-UR-99-4676

Los Alamos National Laboratory is operated by the University of California for the United States Department of Energy under contract W-7405-ENG-36.

TITLE: Puff Meander Model: User's Guide

AUTHOR(S): Michael J. Brown

SUBMITTED TO: General Distribution

By acceptance of this article, the publisher recognized that the U S Government retains a nonexclusive, royalty-free license to publish or reproduce the published form of this contribution or to allow others to do so for U S Government purposes.

The Los Alamos National Laboratory requests that the publisher identify this article as work performed under the auspices of the U S Department of Energy.

Puff Meander Model:
Users Guide

Developed for the JBREWS Project

Michael J. Brown
Los Alamos National Laboratory
Group TSA-4, MS F604
Los Alamos, NM 87545

last revision: 8/19/99

I. Introduction

A puff meander dispersion model has been developed to simulate an airborne aerosol release as part of the Joint Biological Remote Early Warning System (JBREWS) Project. The main goal of the JBREWS Project is to provide rapid warning to U.S. troops of an airborne biological agent attack. One part of the system is fast-response particle-size counters placed in the vicinity of the troops that monitor for "suspicious" aerosol events. Algorithms are being developed to help determine whether the "suspicious" event is a possible biological agent cloud or just naturally-occurring background atmospheric particles. These detection algorithms use the particle-count time-series data collected from numerous particle counters placed in the field. Field tests were performed at the Dugway Proving Grounds in order to test the detection algorithms, but time and fiscal constraints limited the number of release types and atmospheric conditions studied.

A wider range of release types and atmospheric conditions may be examined with artificial datasets. To do this, we developed and applied a puff meander model to produce artificial datasets of particle count time series. These simulated particle count time series were then superimposed onto background aerosol measurements and used to further test the detection algorithms. The puff meander model allows for many source types, agent size distributions, and atmospheric conditions to be tested in a relatively short amount of time. A meander model was chosen, as opposed to the traditional ensemble mean Gaussian model, because real plume dispersal in the atmosphere is semi-chaotic (see Fig. 1) and the resulting time series of concentration (or particle count) at any sensor is characterized by a fluctuating signal. The traditional ensemble mean Gaussian dispersion model only computes the average concentration, whereas the puff meander model has the capability of producing a time-varying fluctuating concentration time series. In principle, a time or ensemble average of the puff meander model output will result in a concentration field similar to that produced by the traditional Gaussian dispersion model.

This report will provide background information on the puff meander model. Specifically, we will describe the mathematical formulation of the model, the limitations (assumptions) inherent in the approach, and the model input requirements. Examples of model output using several real datasets will be provided. Sensitivity of the model to input parameters will be discussed as well. Rigorous validation of the model has not yet been performed. The puff meander model is a sim-

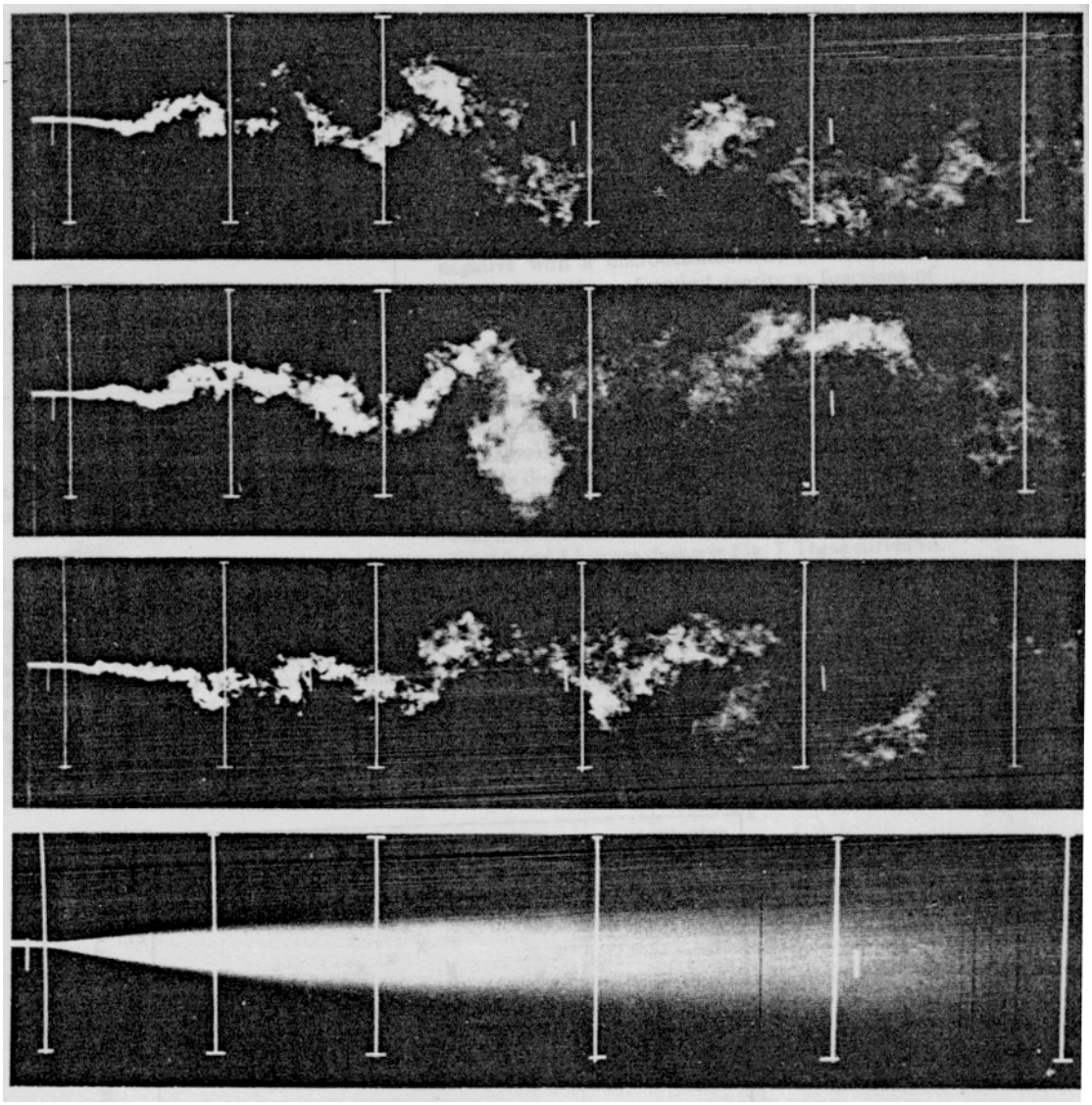

Figure 1. Plume dispersal in a wind-tunnel simulated atmospheric boundary layer. The top three photos show the intermittent nature of instantaneous plume dispersion. The last photo shows a time-averaged plume (produced with a long time exposure). In principle, the puff meander model can capture some of the variability found in the top three photos. The traditional ensemble-mean Gaussian dispersion model produces concentration fields more like the time-averaged plume at bottom.

ple model that runs quickly and can capture the general features of concentration fluctuations. It is not a high fidelity model, however, and users should exercise caution in applying it outside the parameter space for which it was designed.

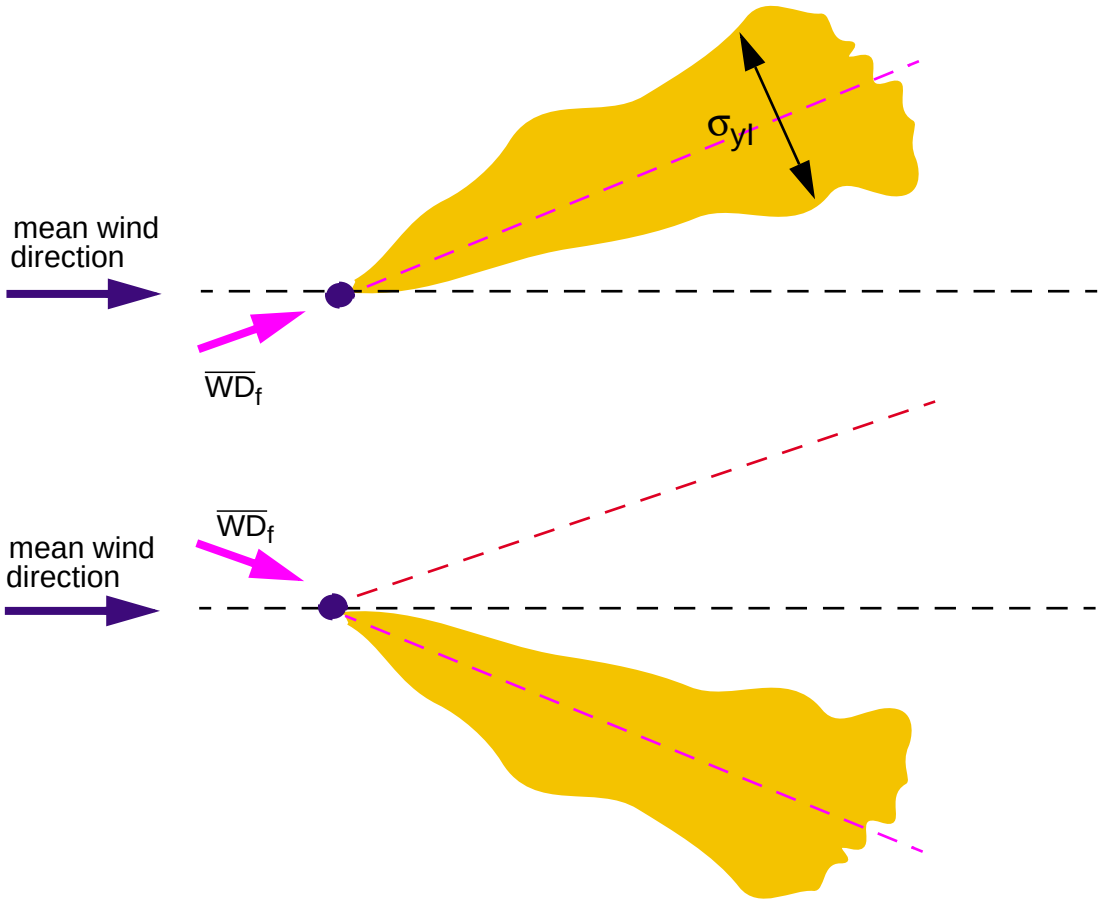

Figure 2. Conceptualization of the plume meander model developed by Peterson and Lamb (1992). The plume position changes as the wind direction changes. In reality, the filtered wind direction WD_f is a function of downwind distance, so that the plume centerline, in general, will not be defined by a straight line as in the drawing.

II. Model Description

Our initial efforts began with a plume meander model developed by Peterson and Lamb (1992). In effect, their model simulates a "flopping" plume that changes position (flops) as the wind direction changes (Fig. 2). The plume shape is described by the Gaussian plume formula with instantaneous plume spread parameters. The model requires a filtered wind direction time series that is a function of downwind distance. The filtered wind direction is fed into the model and as the wind direction changes the plume centerline aligns with the wind (see Fig. 2). In comparisons to field data, Peterson and Lamb (1992) and Donovan and Peterson (1997) showed that the model reasonably simulates the real-time behavior of the fluctuating plume. The model equations and a few examples of model output are given in Appendix A.

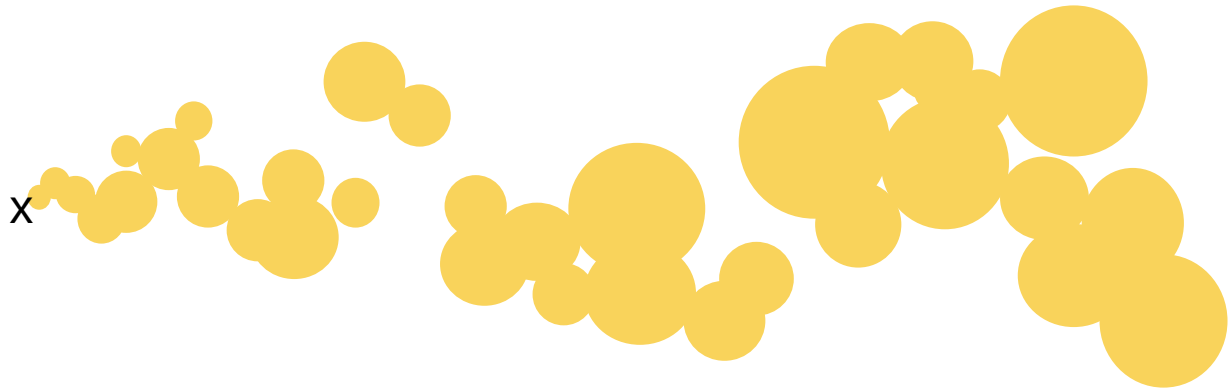

Figure 3. Conceptualization of the puff meander model. A series of "instantaneous" puffs are released from the source x. The puff position changes as the wind direction changes. The meander approach requires knowledge of the wind direction time series. In addition, the width of each puff must be described by an instantaneous puff width, not the traditional ensemble mean plume widths (e.g., Pasquill-Gifford σ_y and σ_z plume spread parameters).

The plume meander model, however, is not appropriate for short-time or instantaneous releases, the type of releases being addressed in the JBREWS Project. Hence, we have modified Peterson and Lamb's plume meander model and created a puff meander model. In this approach, a series of puffs are released and transported with the time-varying wind (Fig. 3). For instantaneous releases, one puff can be released and tracked with downwind distance. For continuous releases, puffs can be released at specified time intervals in order to mimic a plume. The puff meander approach has additional advantages over the plume meander approach: it can better simulate the snake-like meandering of the plume, it can incorporate spatially- and time-varying network winds, it can account for vertical wind shear, and the time-consuming wind direction filtering can possibly be disregarded. The disadvantages include needing to define the longitudinal instantaneous puff spread parameter σ_{xi}, potentially having to track many puffs, and possibly having to interpolate wind sensor measurements.

a. Model Equations

The puff meander model equations are very similar to the traditional ensemble mean puff dispersion models, except that the puff spread parameters σ_{xi}, σ_{yi}, and σ_{zi} are instantaneous values. The concentration distribution for each puff is described by the Gaussian formula:

Equation 1. Puff concentration distribution.

$$C_{puff}(x, y, z, t) = \frac{Q}{(2\pi)^{3/2}\sigma_{xi}\sigma_{yi}\sigma_{zi}} \exp\left\{-\frac{1}{2}\cdot\left[\frac{(x_C - x)^2}{\sigma_{xi}^2} + \frac{(y_C - y)^2}{\sigma_{yi}^2} + \frac{(z_C - z)^2}{\sigma_{zi}^2} + \frac{(z_C + z)^2}{\sigma_{zi}^2}\right]\right\}$$

where Q is the source strength. The last exponential term accounts for reflection at the ground surface. The total concentration is then obtained by summing over all puffs:

Equation 2. Total concentration at any point in space and time (x, y, z, t).

$$C(x, y, z, t) = \sum_{puff\ =\ 1}^{total\ puffs} C_{puff}(x, y, z, t)$$

The horizontal puff centroid location (x_C, y_C) is obtained at each time step by using the current wind speed components U and V and updating the old centroid location:

Equation 3. Puff centroid location.

$$x_C(t) = U(t)\cdot\Delta t + x_C(t - \Delta t)$$

$$y_C(t) = V(t)\cdot\Delta t + y_C(t - \Delta t)$$

Currently, the height of the puff center z_C is assumed to remain at the same height as the initial release height. For daytime simulations, this is a poor assumption, but for stable nighttime conditions, the vertical motion of the puff is expected to be suppressed.

The key parameters to define are the instantaneous puff spread parameters σ_{xi}, σ_{yi}, and σ_{zi}:

Equation 4. Instantaneous puff spread parameters.

$$\sigma_{xi} = \sigma_{yi} = f_1\cdot\sigma_\theta\cdot r$$

$$\sigma_{zi} = f_2\cdot\sigma_\phi\cdot r$$

Here they are related analogously to the ensemble mean puff spread parameters which are a function of the downwind distance r and the standard deviation of the horizontal and vertical wind direction components, σ_θ and σ_ϕ, respectively (e.g., see Boubel et al., 1994). The f_1 term has been determined empirically by Peterson and Lamb (1992) as equal to 0.2224. Fewer simultaneous measurements have been made of the instantaneous vertical puff spread and the vertical wind direction standard deviation. Researchers have instead related measurements of the instantaneous horizontal puff spread to the vertical puff spread, getting around the need to measure σ_ϕ directly and know f_2. Peterson and Lamb (1995) found that σ_{yi} and σ_{zi} were related by a constant, while Turner (1994) reports that σ_{yi} and σ_{zi} are related by a stability-dependent function:

Equation 4a. Peterson and Lamb (1995) σ_{yi} and σ_{zi} relationship

$$\sigma_{zi} = \sigma_{yi} / 4.5$$

Equation 4b. Turner (1994) σ_{yi} and σ_{zi} relationship

$$\sigma_{zi} = \left(\frac{c \cdot r^{d}}{a \cdot r^{b}} \right) \cdot \sigma_{yi}$$

The constants a, b, c, and d can be found in Appendix B.

b. Model Input Parameters and Options

The puff meander model requires the source term, stability conditions, simulation time, wind input files (wind speed, wind direction and σ_θ time series), receptor locations, and a grid definition. Figure 4 shows the input file. The first eight lines describe the source term. The location of the source (the puff release point) is defined by the east-west location XS and the north-south location YS. The source location must be specified in kilometers. Note that the coordinate system is arbitrary, but should agree with the coordinate system used to define the receptor locations and the concentration grid. The height of release is specified through ZS and defines the center of the puff at the release location. Note that ZS is the height above ground level and is specified in units of meters. The initial size of the puffs are defined by SIGY0 and SIGZ0 in units of meters. The initial puff concentration distribution is assumed to be described by Eqn. 1 with $\sigma_{xi} = \sigma_{yi} =$

```
0.02667  ! QS          = source strength (release rate, kg/s)
30.      ! QT          = puff release duration (s)
27.      ! QHR         = puff release start time (lst, 12-36 hrs)
10.0     ! SIGY0       = initial horizontal puff size (m)
10.0     ! SIGZ0       = initial vertical puff size (m)
326.     ! XS          = E-W source location (km, utmx coord.)
4437.    ! YS          = N-S source location (km, utmy coord.)
10.      ! ZS          = release height (m)
2        ! ISIGTHET    = 1 raw sigma theta data; =2 smoothed sigma theta data
2        ! IWIND       = 1 no ws variation w/ ht; =2 ws variation w/ ht.
0.0      ! WD_SHEAR    = degs. of wind direction change per 10 meters height
0.0      ! WD_CRCTN    = error in dugway wd's due to using magnetic north
2        ! ISIG        = 1 sigzi=sigyi; =2 sigzi from Turner
E        ! ASTABILITY  = stability class (A-G): used if IWIND=2 or ISIG=2
1        ! NSENSORS    = no. of input files (sensors) to read in
wind.mean12           != name of mean wind input files (# of lines = NSENSORS)
wind.stat12           != name of sigma theta input files (# of lines = NSENSORS)
10.      ! DT_WIND     = wind data spacing (s)
45.      ! SIM_TIME    = simulation time after release start (min)
12       ! NRCPTRS     = no. of receptors
1.0      ! Zr          = receptor height (m)
#
# E-W location of receptors (km, utmx coord.)
#
 $XRCPTRS
 XR=
 322.785,
 323.269,
 323.848,
 324.257,
 324.564,
 324.423,
 323.953,
 323.486,
 323.099,
 322.729,
 323.410,
 323.942
 $END
#
```

```
# N-S location of receptors (km, utmx coord.)
#
 $YRCPTRS
 Yr=
 4438.580,
 4438.968,
 4438.918,
 4438.407,
 4437.994,
 4437.368,
 4437.003,
 4437.129,
 4437.591,
 4438.018,
 4438.191,
 4437.544
 $END
1        ! IGRD        = compute conc's on grid = 1, otherwise -9
322.5    ! UTMW_GRD    = western bound of grid (km)
4437.0   ! UTMS_GRD    = southern bound of grid (km)
60       ! NGRDX       = no. of grid points in E-W direction
50       ! NGRDY       = no. of grid points in N-S direction
0.05     ! DGRD        = grid size (km)
1.0      ! ZGRD        = height agl of conc. computations (m)
120.     ! T_PRNT_GRD  = time interval between conc. grid print dumps (s)
```

Figure 4. The puff meander model input file.

SIGY0 and σ_{zi} = SIGZ0. The start time of puff releases is defined by QHR and the length of time the puffs are released over is defined by QT. QHR is used to loop through the input wind data to the appropriate time. The total mass released during the release is the product of the source strength QS and the release duration QT. One puff is released at each simulation time interval. Currently, the simulation time interval is equal to the time interval between subsequent wind measurements (defined as DT_WIND). The value of DT_WIND is, of course, dependent on the sampling rate of the wind sensor measurements being used as input to the model.

The next six lines (lines 9-14) are meteorological options. The parameter ISIGTHET is set to 1 if the wind direction fluctuation data being input to the model are representative of instantaneous values ($\sigma_{\theta i}$) and is set to 2 if the data are representative of the time-averaged values (σ_{θ}). The former are obtained by measuring the instantaneous puff spread ($\sigma_{yi} = \sigma_{\theta i} * r$) and therefore are not usually used. The latter are obtained by computing the standard deviation of the wind direction time series measurements.

The next two parameters, IWIND and WD_SHEAR were added to the model because the wind data we are using were measured at one height only. Since the winds typically vary with height, these options might be beneficial if the release height ZS is different than the wind speed measurement height ZM. The IWIND option is set to 1 if the input wind speed measurements are assumed to be constant with height and is set to 2 if the wind speed is assumed to vary with height as a stability-dependent power-law profile (see Appendix C). This option uses the ASTABILITY parameter to define the Pasquill-Gifford stability class. The WD_SHEAR parameter defines the change in wind direction per every ten meter change in height. This parameter is useful if one knows that the wind direction is different between the release height and the wind measurement height. Without knowledge of the wind direction shear, it is best to set WD_SHEAR = 0.

The next parameter, WD_CRCTN, was added to the input file to adjust the wind directions being read in from the mean wind input file. A positive value adds to the measured wind direction, a negative value reduces the measured wind direction. This correction was needed for our particu-

lar case because the wind direction data were reported relative to magnetic north, not true north. The ISIG parameter is set to 1 if Eqn. 4a is used to relate σ_{yi} and σ_{zi} and is set to 2 if Eqn. 4b is used. Appendix B lists the specifics of the parameters in Eqn. 4b. The ASTABILITY parameter is the Pasquill-Gifford stability class (A - unstable, B - unstable, C - slightly unstable, D - neutral, E - slightly stable, F - strongly stable) (e.g., see Boubel et al, 1994; Turner, 1994) and is used to define the power-law profile shape parameters (IWIND = 2) and the σ_{yi}/σ_{zi} relationship defined in Eqn. 4b (ISIG = 2).

Next, the number of input files (wind sensors) NSENSORS is specified, the names of the wind input files are given (one for wind speed and direction time series and one for the wind direction standard deviation time series data), and the time increment of the wind measurements DT_WIND is specified. The format of the wind sensor input files will be discussed in Section III. Although the puff meander code has been dimensioned to accept multiple wind sensor input files, no algorithm has been incorporated into the code for interpolating between measurements. Hence, NSENSORS should be set to 1. The SIM_TIME parameter determines how long the simulation runs for (i.e., how long the puffs are tracked for). It can be longer (or shorter) than the release duration QT.

The next parameters define the receptors (the locations at which the concentration time series are computed). NRCPTRS is set to the number of receptors desired (currently 100 maximum). The height of the receptors is specified in meters above ground level through Zr. The location variables XR and YR are specified in the namelists XRCPTRS and YRCPTRS, respectively. The locations in kilometers for receptors 1 - NRCPTRS is given sequentially, first for the east-west coordinate (XR) and then for the north-south coordinate (YR).

The next set of parameters are used to delineate a grid over which to compute concentrations. One could define a grid by appropriately defining the receptor locations above, but it is much quicker to do so here. The IGRD option is set to 1 if the user desires to compute concentrations on a grid and is set to -9 if the user does not desire to do so. The next six variables define the grid.

UTMW_GRD denotes the western edge of the grid and UTMS_GRD denotes the southern edge. Note that the utm coordinate system does not need to be used. The number of grids in the east-west and north-south directions is represented by NGRDX and NGRDY, respectively. The grid size in kilometers is defined by DGRD and the height of the grid in meters above ground level is defined by ZGRD. Finally, the print interval at which to compute and print out the concentration grid is defined by T_PRNT_GRD. The units of T_PRNT_GRD are in seconds and should be an even multiple of the wind measurements time increment DT_WIND.

c. Limitations

There are numerous approximations in the puff meander code that limit its range of applicability. Some are inherent in the equations and would be difficult to overcome (one could develop higher fidelity models, e.g., a large eddy simulation computational fluid dynamics code, but these have the downside of being extremely computationally expensive and could not be used to do many analyses in a short amount of time). In addition, there are many "bells and whistles" that haven't been added yet, but could be added if further development is supported. Below, we list some of the major shortcomings of the puff meander model.

There are several limitations associated with the form we have assumed for the puff. First, the concentration within the puff is assumed to have a Gaussian distribution. In the real world, even for a highly idealized source release, the puff can be non-Gaussian. One could, however, define the source distribution by several Gaussian puffs that in summation results in a non-Gaussian source. Second, the concentration within the Gaussian puff is assumed to vary smoothly from one side of the puff to the other. In the real world, the concentration across the puff will not be smooth, i.e., there will be in-puff concentration fluctuations. We are assuming that the bulk of the concentration fluctuations seen at a sensor are caused by the meander of the puff or plume across the sensor, not by the small-scale in-puff fluctuations. Third, as the puff grows larger the top part of the puff, in the real world, can travel at a different speed (usually faster, since the winds are generally faster higher up) than the bottom part of the puff. Currently, our puff meander code does not account for this. Typically, this is accomplished by puff splitting, i.e., when the puff gets too large, it is split into smaller puffs.

There are a number of approximations contained in the computation of the puff trajectories. First, as the puff travels with the wind, the puff center remains at the same height. During nighttime conditions where it is stably stratified, this assumption might be ok. But for the daytime, when convection occurs, the puff can be transported large vertical distances by convective eddies. In principal, vertical motion could be accounted for in the model if we had measurements of vertical wind speed. The effect of the enhanced vertical mixing, however, is accounted for in the puff spread parameters σ_{xi}, σ_{yi}, and σ_{zi}. Second, because the puffs stay on one height level, there is no attempt to account for wind variation with height (except through the source term, as described earlier). In principal, puffs can be released at different heights using winds measured at the different heights, and then by summing together the concentrations from the different puffs account for the impact of wind shear on transport and dispersion. Third, the trajectories do not account for terrain obstacles, in effect, the puffs are assumed to be released over flat topography. In principal, the impact of terrain obstacles could be accounted for if there were enough measurements around the obstacle to accurately describe the flow field. However, the puff meander model currently does not have a wind interpolation scheme to utilize such data. In addition, any stretching or distortion of the puff as it interacted with the terrain obstacle would not be accounted for.

As we have already mentioned, there currently is no wind interpolation scheme in the code. That means we cannot currently utilize multiple wind sensors for advecting the puffs. Over large transport distances or in regions of complex terrain, using only one wind sensor to define the transport of the puff is not acceptable since the wind characteristics are expected to be horizontally inhomogeneous. In addition, the code is dependent on the sampling time of the wind measurements. Low frequency wind measurements may give poor results. The narrower the puff or plume, the higher the frequency needed to capture the meander of the tracer release. It is not clear, *a priori,* what sampling time is required for a particular problem. Furthermore, we have found that the calculation of the wind direction standard deviation σ_θ is sensitive to the averaging time. Again, it is not clear what averaging time is the “right” averaging time, i.e., the one that reproduces the important physics most accurately.

Also of concern is that the plume spread parameters themselves are not well characterized. The measurements that are available are sparse and therefore the uncertainty in the formulae may be large. Finally, deposition, resuspension, and degradation processes are not accounted for in this version of the puff meander code. These processes may be significant depending upon the nature of the particle or agent released, the meteorological conditions, or the plume travel time.

III. Pre- and post-processor routines (developed for Dugway field trials)

A number of pre- and post-processor programs have been developed for various data conversion needs. Figure 5 shows the various programs in flowchart format. The codes and data files in the gray box are the essential components for producing concentrations and particle counts with the puff meander model. The programs and data files outside the gray box were developed specifically for the Dugway field trial datasets. These would have to be modified for other datasets.

The puff meander model (current version 1.5) requires three input files: the puff_input file described above, a wind components data file, and a wind direction statistics data file. The essential variables needed from the two wind measurements data files are the time (hours), wind speed (m/s), wind direction (degrees), and the wind direction standard deviation σ_θ (degrees). Currently, the puff meander code is set up to read the wind components data file in the following format: time, wind speed, wind direction, U velocity component, and the V velocity component. It also reads several header lines. Figure 6a shows the first part of a typical wind components input file. The wind direction statistics input file is currently read in as: time, σ_θ, σ_u, and σ_v. Figure 6b shows the first few lines of a typical wind direction statistics input file. The header information in both wind input files give information on the source of the data file, number of lines in the data file, averaging times of the data, and column labels. The number of running averages, the averaging times, the variance averaging time, the wind direction running average time, and the number of lines are required by the puff meander code. These values are produced automatically by the pre-processor codes described below.

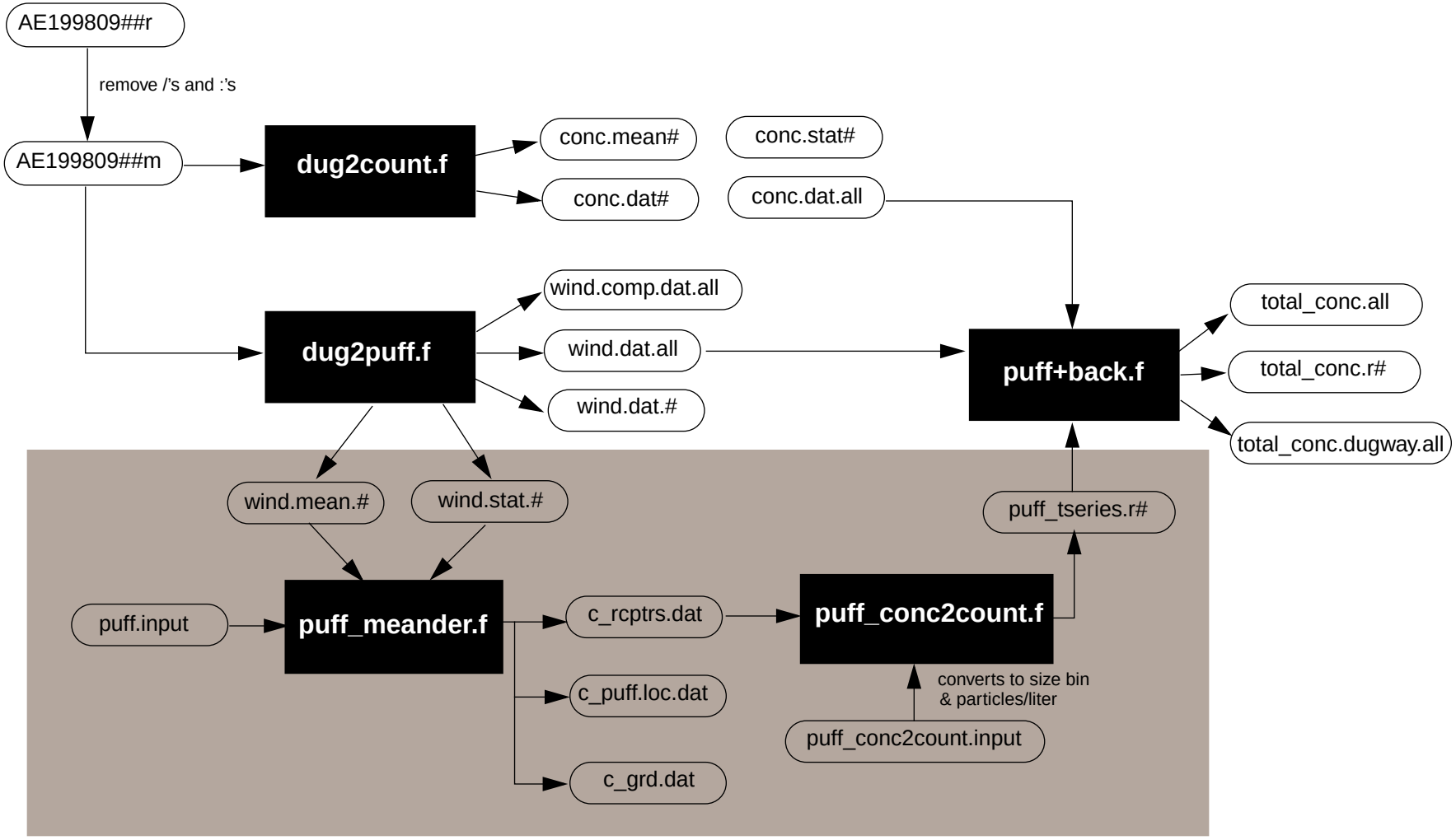

Figure 5. The puff meander model input files, pre-processors, and post-processors. The codes and data files in the gray box are the essential components for computing concentrations and particle size bin counts with the puff meander model. The codes and data files outside the gray box were developed specifically for the Dugway field trials and consist of pre-processors for getting the data in the right format for the puff meander code and a program for adding the measured background particle counts to the simulated tracer particle counts.

a)

```
SENSOR #  1
 INPUT FILE = AE19980902m
  5 = NO. OF RUNNING AVERAGES
   10.00000 S = AVERAGING TIME
    180.000 S = AVERAGING TIME
    300.000 S = AVERAGING TIME
    600.000 S = AVERAGING TIME
    900.000 S = AVERAGING TIME
 2530 = NO. OF LINES
 RUNNING AVERAGE TIME (S) =   10.00000
 TIME  WSavg  WDavg  Uavg  Vavg   NPTS
    23.0027   0.600026    115.002  -0.543800   0.253600  1
    23.0054   0.600026    115.002  -0.543800   0.253600  1
    23.0082   0.900039    115.002  -0.815700   0.380400  1
    23.0110    1.20001    114.998   -1.08760   0.507100  1
    23.0138   0.699972    114.998  -0.634400   0.295800  1
    23.0165   0.600026    115.002  -0.543800   0.253600  1
    23.0193   0.799960    115.002  -0.725000   0.338100  1
    23.0221   0.699972    114.998  -0.634400   0.295800  1
    23.0249    1.20001    114.998   -1.08760   0.507100  1
    23.0277    1.20002    115.997   -1.07860   0.526000  1
    23.0304    1.00002    116.001  -0.898800   0.438400  1
    23.0332   0.899972    115.998  -0.808900   0.394500  1
    23.0360    1.00002    116.001  -0.898800   0.438400  1
   ...
```

b)

```
SENSOR #  1
 INPUT FILE = AE19980902m
    300.000 S = VARIANCE AVERAGING TIME
    180.000 S = WD RUNNING AVERAGE TIME
 2530 = NO. OF LINES
 TIME  SIGTHETA  SIGMAUt  SIGMAVt  NPTS
  23.0027    1.61158E-02    7.48942E-02    1.70066E-04  30
    23.0054    3.32002E-02    8.06101E-02    3.48316E-04  30
    23.0082    5.18278E-02    8.29690E-02    7.15671E-04  30
    23.0110    7.29234E-02   0.109183    1.29100E-03  30
    23.0138    9.47079E-02   0.109578    1.48721E-03  30
    23.0165   0.118050   0.118686    1.66024E-03  30
    23.0193   0.142687   0.119411    2.00220E-03  30
    23.0221   0.169095   0.122663    2.28861E-03  30
    23.0249   0.196849   0.133920    3.11334E-03  30
    23.0276   0.210214   0.142159    3.47553E-03  30
    23.0304   0.220195   0.142521    3.65895E-03  30
    23.0332   0.227171   0.141579    3.76272E-03  30
    23.0360   0.233594   0.140646    3.88068E-03  30
   ...
```

Figure 6. a) Wind components input file and b) wind direction fluctuation statistics input file for the puff meander model.

```
c_rcptrs.dat      != concentration time series data input file name
1                 ! IUNITS     = particle no./liter = 1, particle no./m3 = 2
4.68              ! MMD        = mass median diameter (microns) - lognormal params
1.94              ! GSD        = geometric standard deviation (microns)
6                 ! NBINS      = no. of size bins for time series
1.0               ! DBIN(1)    = diameter for size bin cutpoints (smallest first)
2.0               ! DBIN(2)    = diameter for size bin cutpoints (microns)
4.0               ! DBIN(3)    = diameter for size bin cutpoints (need nbins+1 values)
6.0               ! DBIN(4)    = diameter for size bin cutpoints
8.0               ! DBIN(4)    = diameter for size bin cutpoints
10.0              ! DBIN(4)    = diameter for size bin cutpoints
25.0              ! DBIN(4)    = diameter for size bin cutpoints
```

Figure 7. Input file for the *puff_conc2count.f* code used to convert the puff meander model concentrations to size bin particle counts.

The puff meander model produces three output files: the first containing the concentration time series at each receptor, the second containing the puff centroid locations as a function of time, and the third (optionally) concentrations on a grid at user-specified time intervals. The concentrations in the *c_rcptrs.dat* file can then be read into the program *puff_conc2count.f* which converts the concentrations to particle counts per size bin based on a source distribution defined in the *puff_conc2count.input* file (see Fig. 7). The first line contains the name of the concentration time series data input file and on the second line the units of the concentrations are given by IUNITS (particle number/liter = 1; particle number/m^3 = 2). Currently, a log-normal distribution is assumed for the particle size distribution. The mass median diameter MMD and geometric standard deviation GSD are the variables that define the lognormal shape. The next parameter, NBINS, determines how many size bins to divide the log-normal distribution into. The cutpoints for each size bin are then defined by the DBIN parameters.

The programs outside the gray box (see Fig. 5) have been developed specifically to convert the Dugway field trial datasets into formats that can be used by the puff meander model. These programs could be modified to accept different data formats. In short, the *dug2count.f* program converts the Dugway particle count data into four different formats: one containing the raw particle count data in a format adapted to plotting programs, a second containing mean particle concentra-

tions over a user-specified averaging time, a third with standard deviation statistics of the particle count, and the fourth containing all particle count data for all sensors. The program *puff+back.f* combines the background measurements (*conc.dat.all*) with the simulated releases (*puff_tseries.r#*). The *dug2puff.f* program converts the Dugway wind data into five different formats: two that are read into the puff meander model, two that are formatted specifically for plotting programs, and one that is read into the *puff+back.f* code. The *puff+back.f* code produces three files, one of which is in the original Dugway format (*total_conc.dugway.all*).

IV. Model Results

In this section we will show some typical model results. We begin by showing a time sequence of concentration contours for a short time release using Dugway wind data. Figure 8 shows a puff at one minute increments traveling downwind. The concentration within the puff is described by a Gaussian distribution, hence the concentrations within the puff are smoothly varying. As described under Limitations (Section IIc.), this is an oversimplification, as the turbulence would act to distort and stretch the puff. Looking at the puff concentration contours, it is difficult to see the effect of meander.

Figure 9 shows a longer time release where many puffs are being tracked. Looking at the higher concentration portion of the plume (reds, yellows, and light blues), one can clearly see the plume meandering as the wind shifts direction. However, one does not see a “clumpy” plume as seen in the wind-tunnel experiment photos in Fig. 1. This is due to both the smooth Gaussian distribution assumed for each puff and using only one wind sensor as input to the model. Winds at different points in space become more decorrelated as the distance between them increases. Using only one wind sensor means that the movement of puffs is highly correlated and hence “clumping” of the plume is not possible. As we discussed in the Limitations section, with an interpolation scheme, more wind sensors could be incorporated into the puff meander code. However, as we show below, there appears to be a mean bias between the different Dugway wind sensors and therefore we decided not to incorporate multiple sensors into the model simulations.

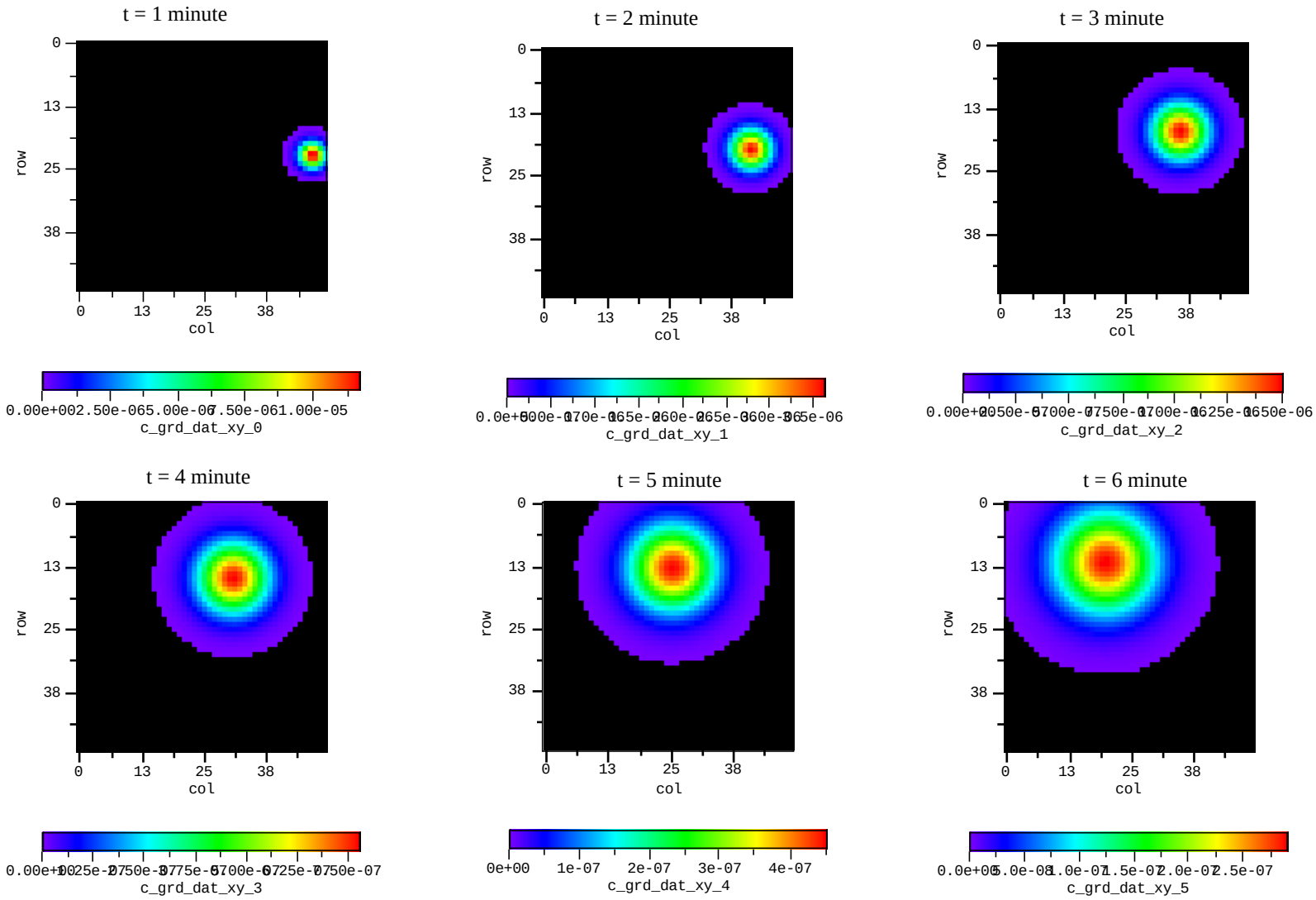

start time = 23.0 hours lst
date = 09/02/98
release duration = 0.5 minute

Figure 8. Concentration contours produced by the puff meander model for a short-time release. Wind data from one Dugway sensor was used to transport the puffs.

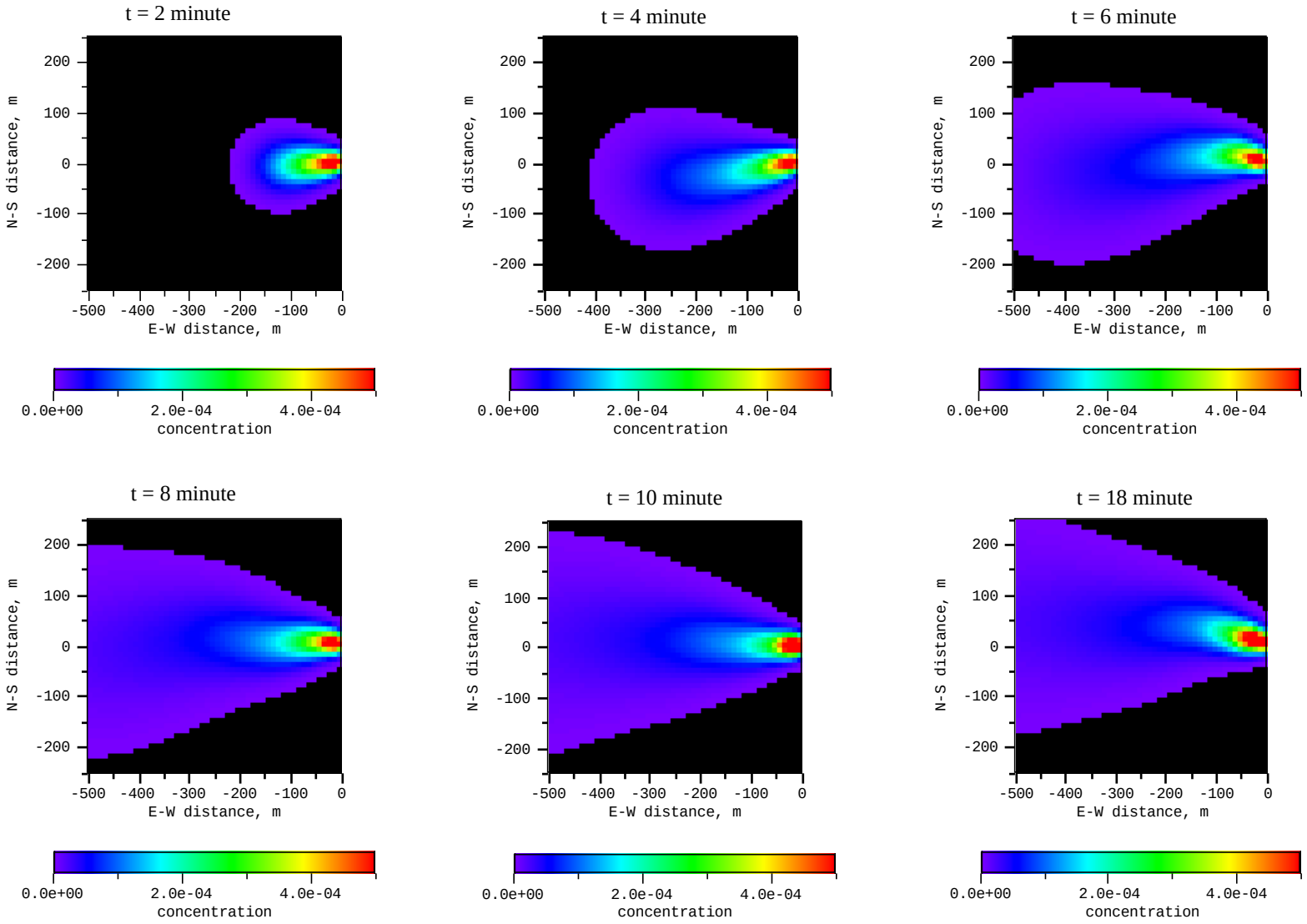

start time = 27.3 hours
date = 09/03/98
release duration = 20 minutes

Figure 9. Concentration contours produced by the puff meander model for a long-time release. Wind data from one Dugway sensor was used to transport the puffs. Notice the "swaying" motion of the plume as the wind direction shifts.

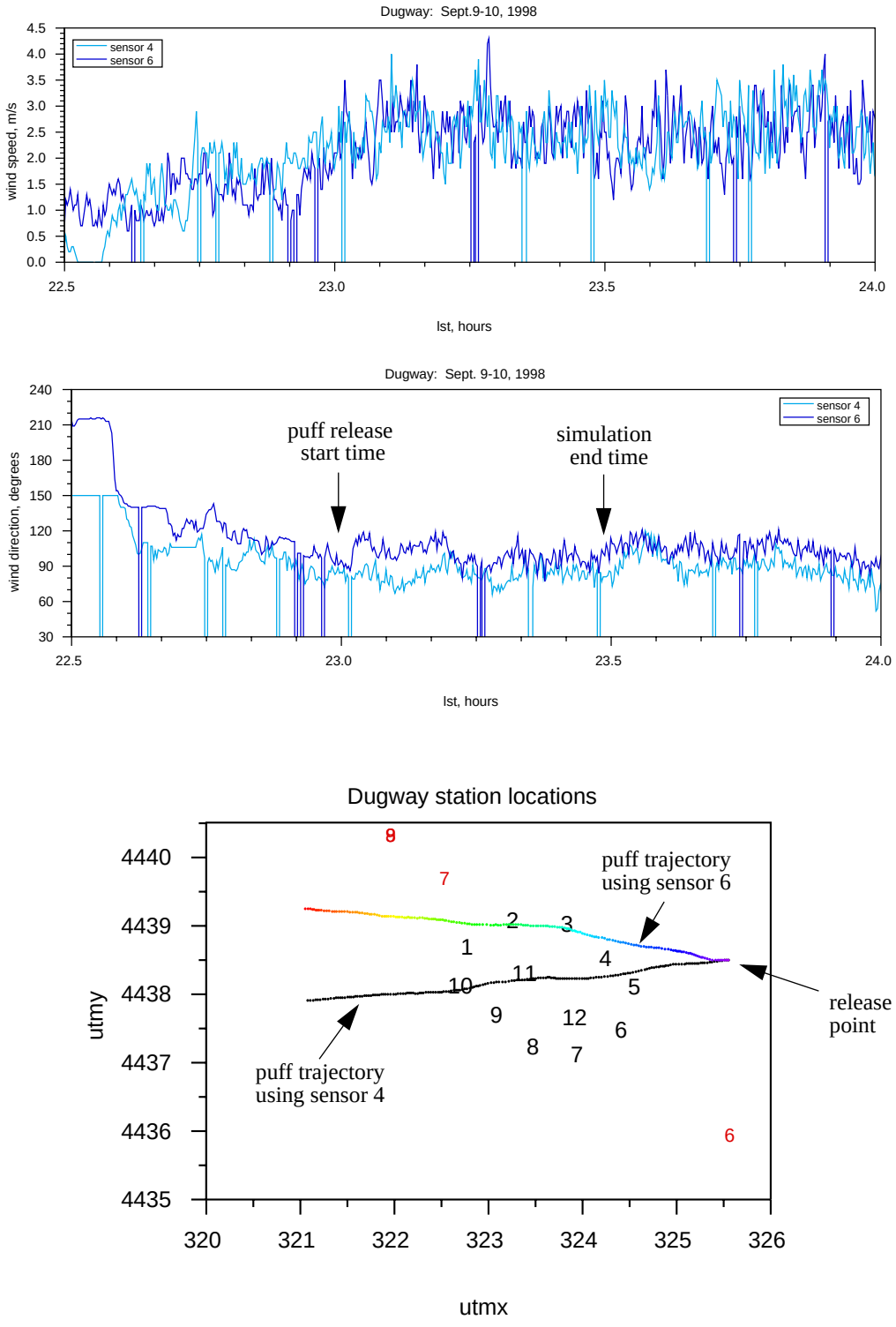

Figure 10. Puff trajectories produced by the puff meander model using two different Dugway wind sensors. Notice that the puffs do not track in straight lines, but rather oscillate as the wind direction varies.

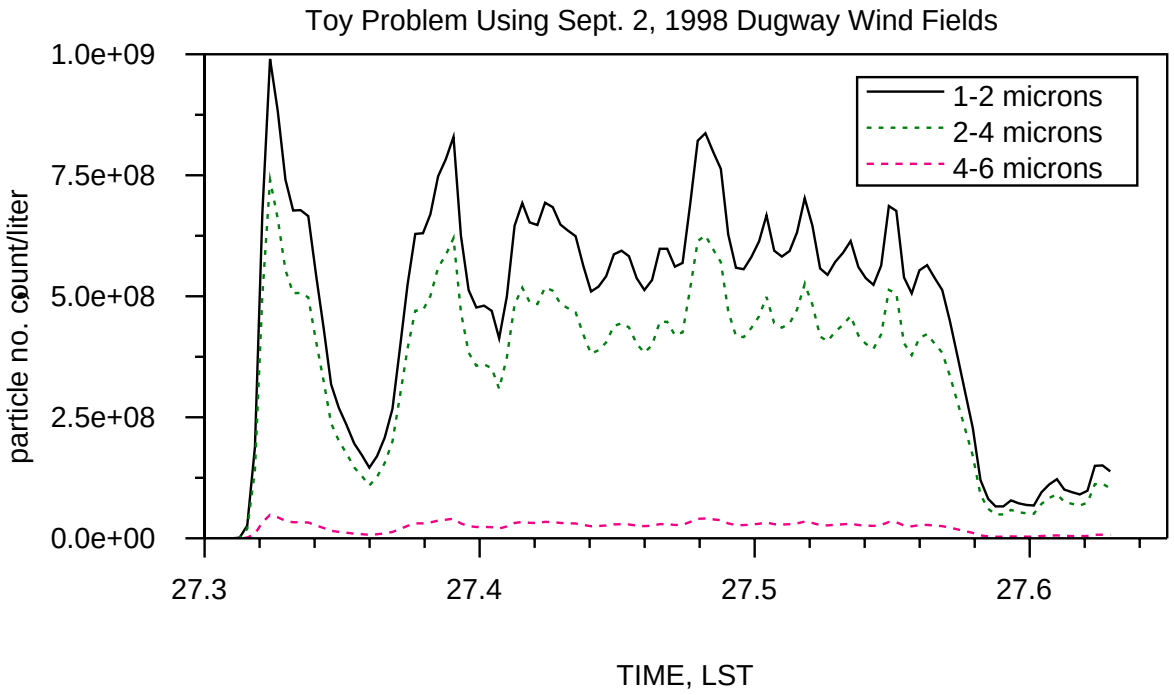

Figure 11. Particle counts in three size bins at a downwind receptor computed by the puff meander model for a finite duration release. The *puff_meander_v1.5* code computed the concentration fields and the *conc2count.f* code computed the particle counts based on a lognormal size distribution with MMD=3.0 microns and GSD = 1.5 microns.

The trajectories of single puffs using two different Dugway wind sensors as input are shown in Fig.10. The release start time for these simulations was 11 pm. One can see that the trajectories shift direction in response to changes in the wind direction. One can also see that small differences in the wind direction result in relatively big changes in the trajectory paths.

An example particle count time series is plotted in Fig. 11. The concentration fields for a finite duration release were computed using the puff meander model using Dugway wind data as input. The *conc2count.f* code was used to transform the data from concentrations to particle counts per liter assuming a log-normal size distribution. The fluctuations in the particle count are a result of the meander of the plume. Notice that the particle counts in each size bin track each other with perfect correlation. Currently, the size distribution is log-normal and contains no stochastic behavior.

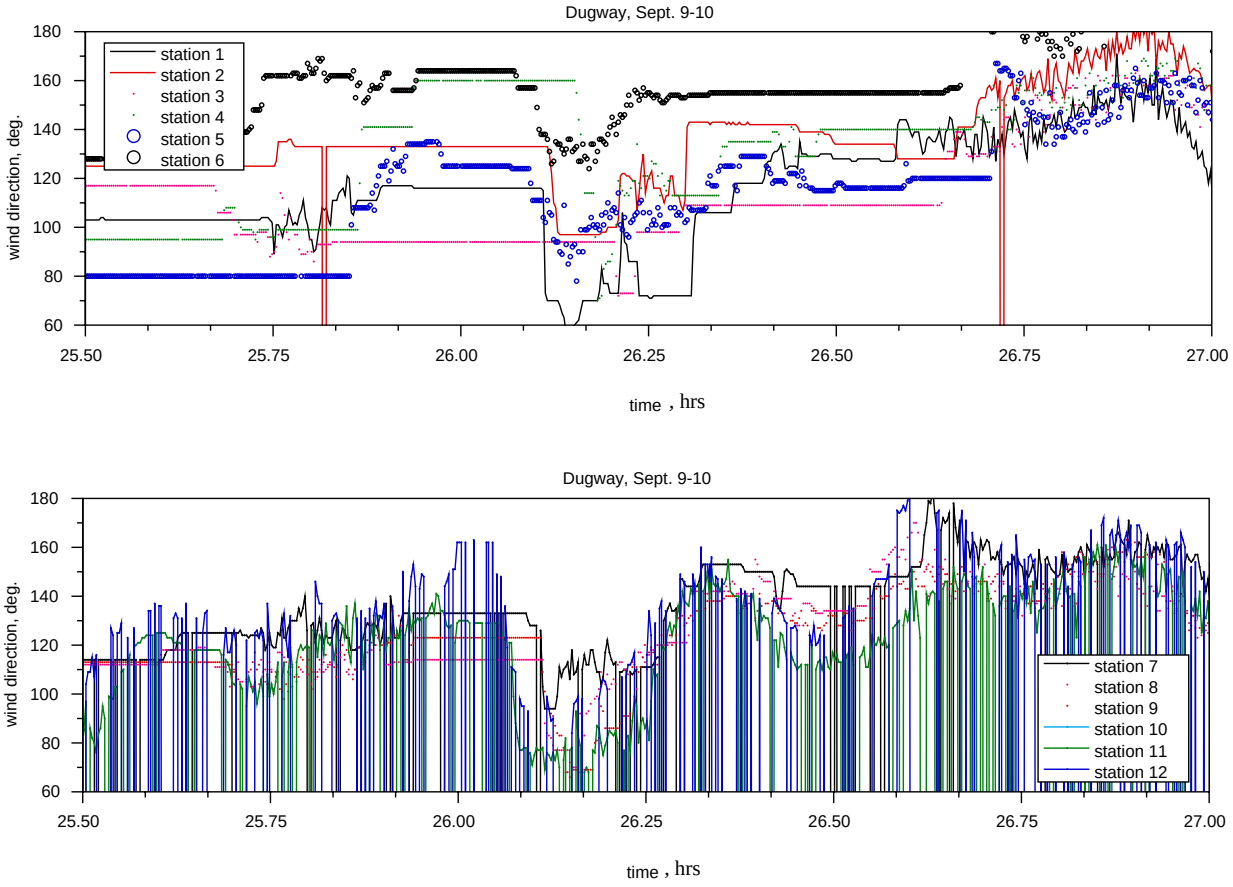

Figure 12. Wind direction measurements for the 12 sensor sites.at the Dugway test site showing significant mean biases between the sensors. The vertical lines denote periods of missing data. The flat horizontal lines are indicative of low wind speeds where the wind sensor has reached it's wind speed threshold (i.e, the winds are too light to move the wind direction vane).

Figure 12 illustrates why we did not attempt to incorporate multiple sensors into the puff meander simulations for the Dugway field trial application. Here, the wind direction measurements from the 12 sensors are all very different even though the sensors are within a few kilometers of one another and there are not significant terrain differences in the area. Although one expects the wind direction to vary between sensors at the same moment in time due to turbulent fluctuations, we see that the mean wind direction is significantly different between stations. This may have resulted because the wind sensors were very close to the ground (1.5 meters above ground level) and therefore were sensitive to slight variations in the topography or it may have been due to poor siting/calibration of the sensors.

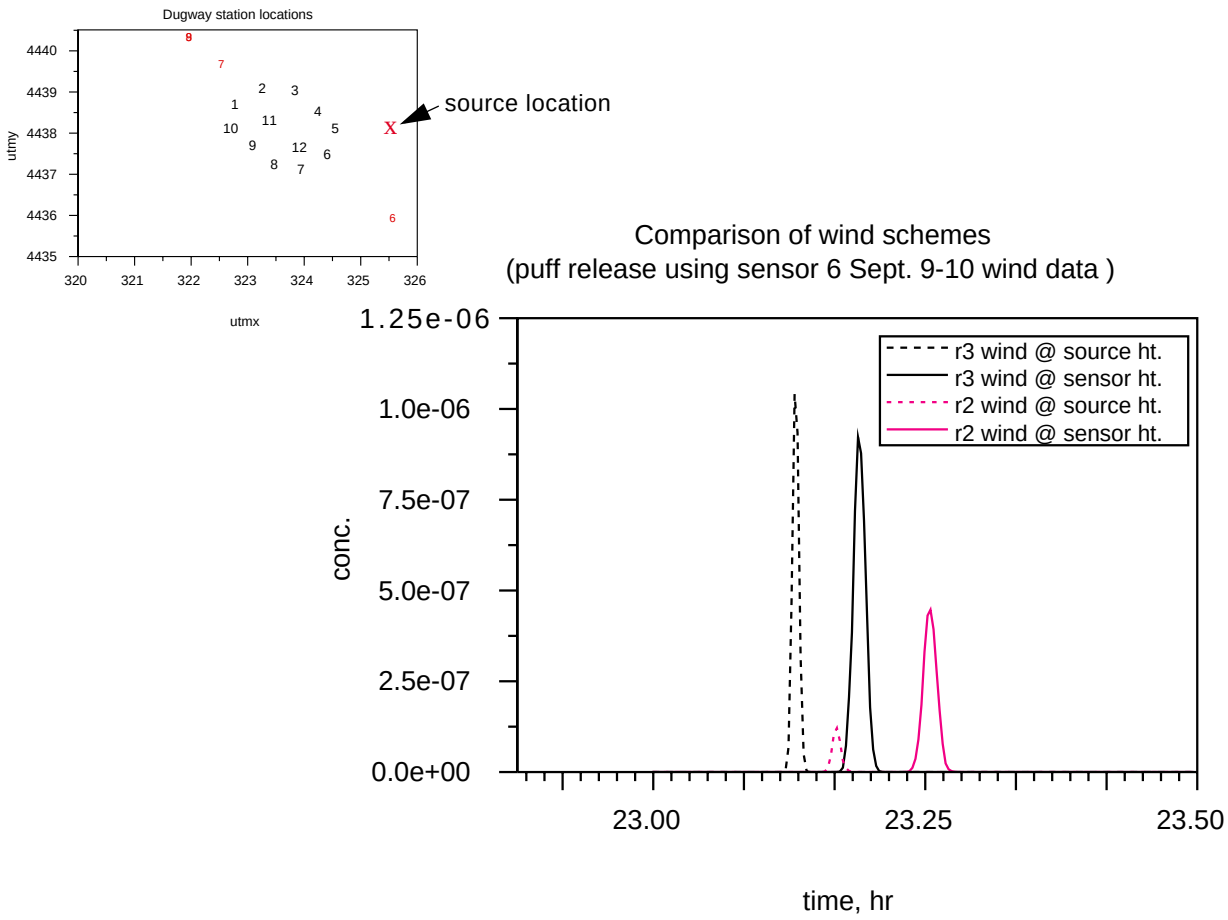

Figure 13. Sensitivity of the puff meander model to the wind scheme. The source height is higher than the sensor height. Winds should be faster at the source height, but we have no wind measurements there. For case 1 (solid lines) the puff is transported using the wind at the sensor height. For case 2 (dashed lines) the puff is transported using a fictitious wind at the release height. This fictitiously wind was computed using the extrapolation scheme described in Appendix C.

The next few figures show sensitivity runs that were performed in order to evaluate the impact of different model parameters and features. Figure 13 demonstrates the impact of the power-law wind profile extrapolation on puff transport and dispersion (see Appendix C). In the first case (solid lines), the puff uses the winds measured at the sensor height even though the release is at a higher elevation. In the second case (dashed lines), an extrapolated wind (extrapolated from the sensor height to the release height) is used to transport the puff. The puff arrives at sensors 2 and 3 five minutes earlier when using the extrapolated (faster) winds. Figure 14 shows the impact of using the different σ_{yi} /σ_{zi} schemes (Eqns. 4a and b). For this case, the concentrations are about a

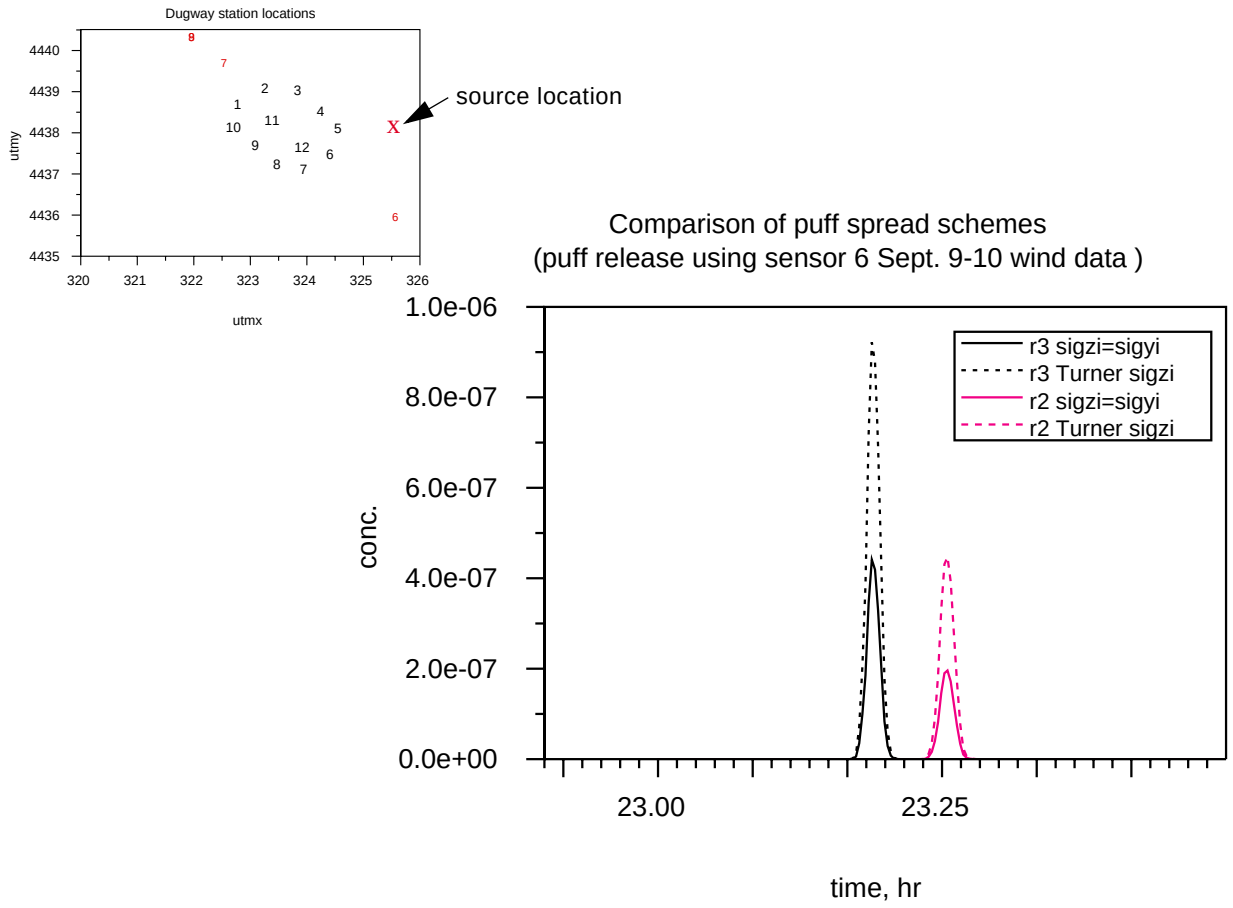

Figure 14. Sensitivity of the puff meander model to the vertical puff spread scheme. The vertical puff spread is defined by Eqn. 4a for case 1 (solid lines) and Eqn. 4b for case 2 (dashed lines). The vertical puff spread for case 1 is proportional to σ_{yi}. For case 2, the vertical puff spread is also a function of stability. Case 2 shows higher concentrations because the puff does not spread as much in the vertical -- and therefore is less diluted -- due to the stable stratification found at night.

factor of two higher when using the stability-dependent Turner scheme (Eqn. 4b). This results from very stable conditions in which the vertical spread of the puff is reduced, and therefore dilution of the puff is small. For convective daytime conditions, the effect might be the opposite, with the Turner scheme yielding smaller concentrations. Numerous other simulations were performed in which parameters were varied, but we will not report these here.

Acknowledgements. Thanks to Tom Wehner for support on this project, to Cathrin Muller for help with some of the figures, and to Jerry Streit, Eric Pardyjak, and Steve Burian for reviewing this document.

References

Arya, S. (1988) Introduction to Micrometeorology, Academic Press.

Boubel, R., D. Fox, D. Turner, A. Stern (1994) Fundamentals of Air Pollution, Academic Press.

Donovan, T. and H. Peterson (1997) Comparison of measured concentration fluctuations to data from a meandering plume diffusion model, 12th AMS Bound. Layer Turb. Conf., Vancouver, BC.

Peterson, H. and B. Lamb (1992) Comparison of results from a meandering-plume model with measured atmospheric tracer concentration fluctuations, J. Appl. Met., v 31, pp 553-564.

Peterson, H. and B. Lamb (1995) An investigation of instantaneous diffusion and concentration fluctuations, J. Appl. Met., v 34, pp 2724-2746.

Turner, D. (1994) Workbook of Atmospheric Dispersion Estimates, Lewis Publishers.

Appendix A. Plume Meander Model Description

In this section, we briefly describe the plume meander model developed by Peterson and Lamb (1992). The ground-level concentration at a point in space is given by:.

$$C(t) = \frac{Q}{\pi \bar{U} \sigma_{yi} \sigma_{zi}} \exp\left[-\frac{1}{2} \cdot \frac{(y_{CL_f} - y_{receptor})^2}{\sigma_{yi}^2}\right]$$

$$= \frac{Q}{\pi \bar{U} \sigma_{\theta i} \sigma_{\phi i} r^2} \exp\left[-\frac{1}{2} \cdot \frac{(\overline{WD}_f - \alpha_{receptor})^2}{\sigma_{\theta i}^2}\right]$$

where Q is the source strength, $\bar{U}$ the mean wind velocity, $\sigma_{yi} = \sigma_{\theta i} * r$ and $\sigma_{zi} = \sigma_{\phi i} * r$ are the instantaneous plume spread parameters, r is the radial distance between the source and the receptor, y_{CLf} is the time-varying plume centerline (assumed to align with the filtered wind direction WD_f), $y_{receptor}$ is the lateral distance from the plume centerline, and $\alpha_{receptor}$ is the angle between the receptor and the plume centerline. The model is set up to compute ground-level concentrations only. The model is basically a “flopping” plume model using a Gaussian distributed plume profile whose centerline changes as the filtered wind direction changes. The wind direction time series is averaged over a time period that is an increasing function of radial distance. Therefore, the plume “flops”, or responds, more quickly to changes in the wind direction near the source as compared to farther from the source. Peterson and Lamb (1992) found that the model was quite sensitive to the filtering time.

The next few examples illustrate the capabilities of the model. Using Dugway wind data, the plume meander model is used to compute a concentration time series at several receptor points (Figs. A1 and A2).

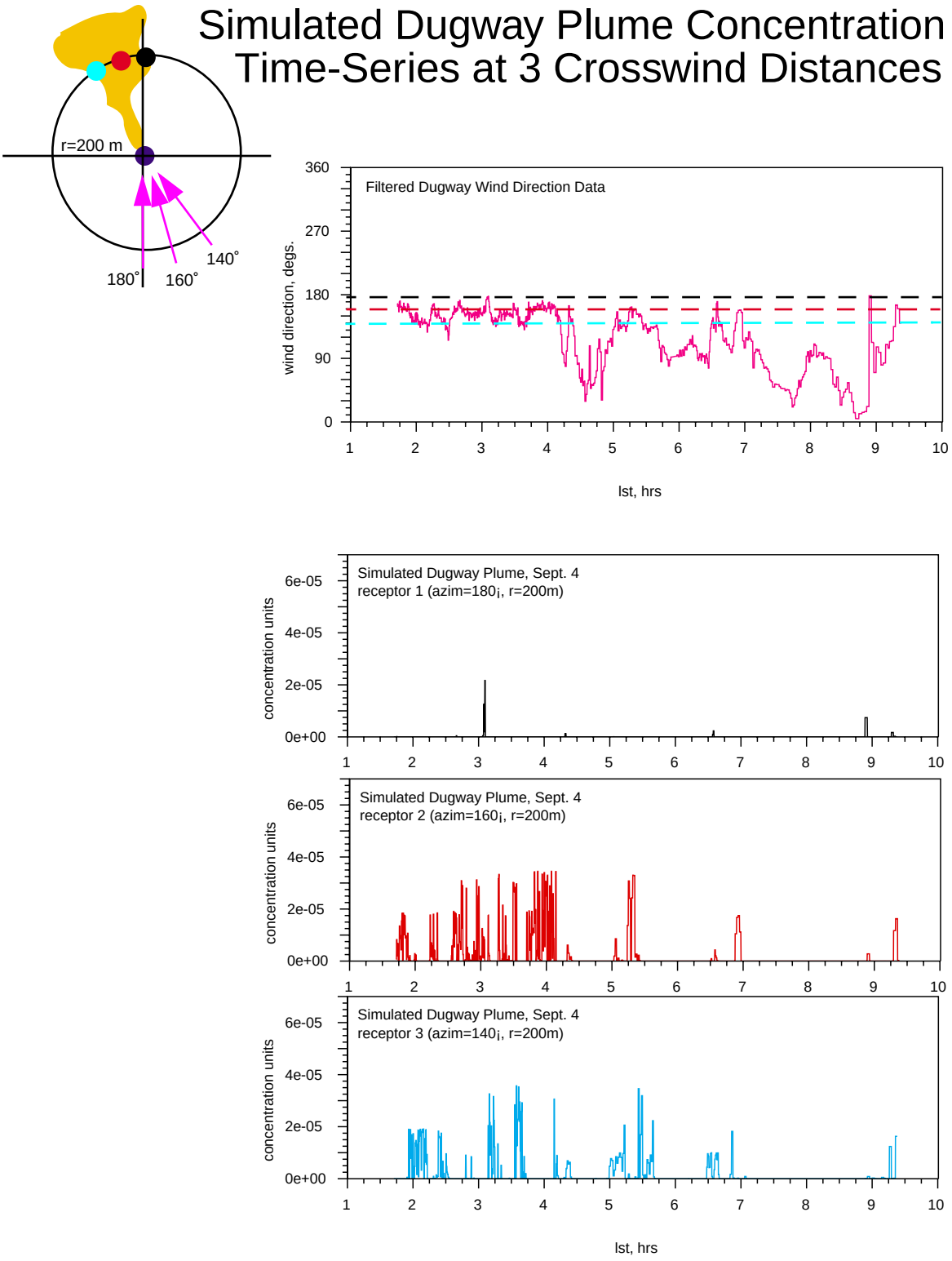

Figure A1. Concentration time series produced by the plume meander model at three receptor sites at the same radial distance and the corresponding filtered wind direction used as input.

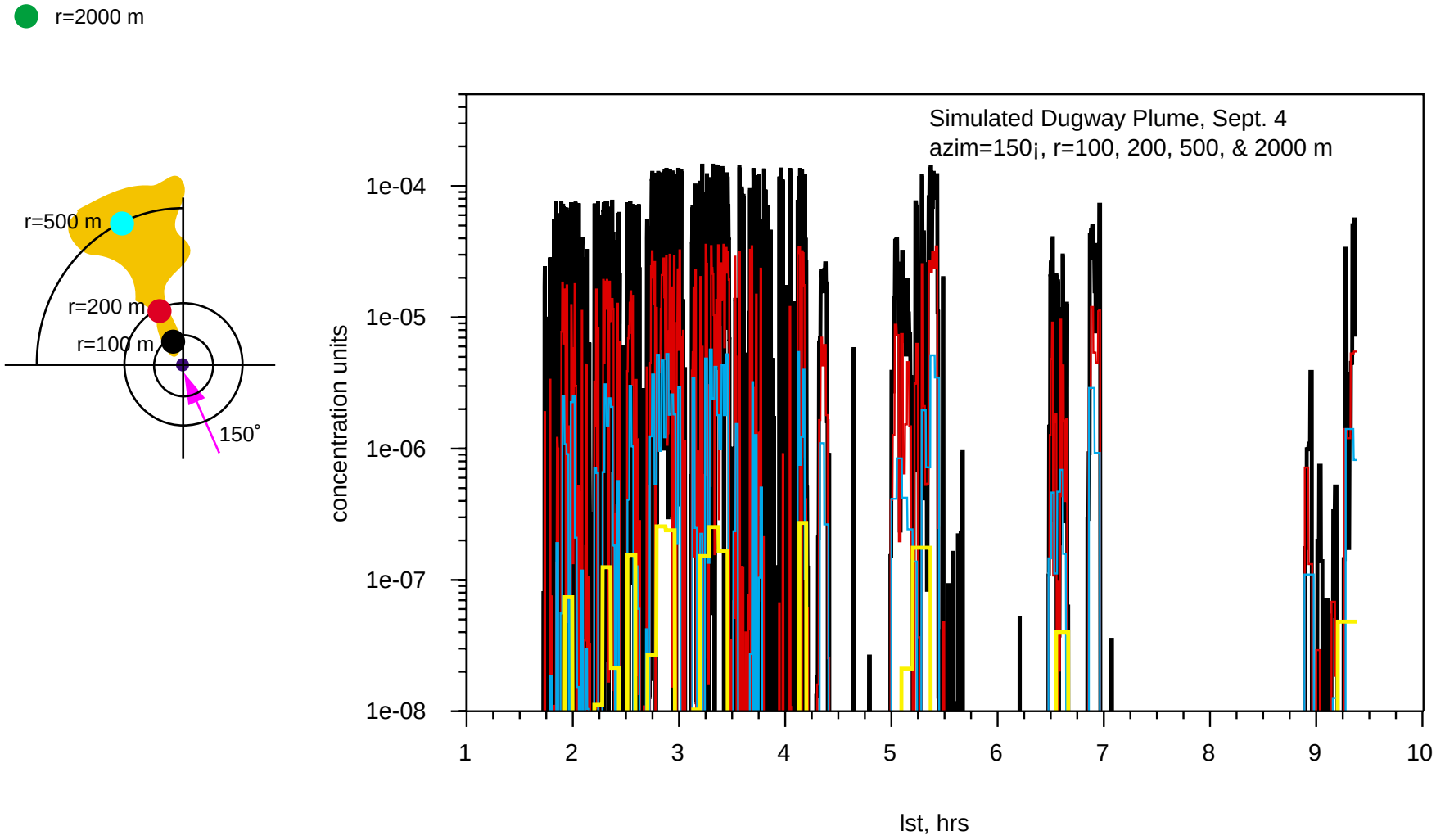

Figure A2. Concentration time series produced by the plume meander model at four different downwind distances. The averaging time for the wind direction increases for larger downwind distances and explains the stair-step nature of the concentration time series at the 2000 m distance.

Appendix B. Turner σ_{yi} and σ_{zi} stability-dependent relationships

We can compute the instantaneous horizontal puff spread parameter σ_{yi} directly from σ_θ measurements. However, the σ_ϕ measurements needed to compute the vertical spread parameter σ_{zi} are often not available. Turner (1995) reported on measurements of σ_{yi} and σ_{zi} as a function of stability. Using these relationships, we can compute σ_{zi} without knowledge of σ_ϕ:

$$\sigma_{zi} = \left(\frac{c \cdot r^{d}}{a \cdot r^{b}} \right) \cdot \sigma_{yi}$$

The variables a, b, c, and d are given in the table below. r is the downwind distance in meters.

Table 1: Instantaneous Puff Spread Parameters

Pasquill Stability	a	b	c	d
A	0.18	0.92	0.72	0.76
B	0.14	0.92	0.53	0.73
C	0.10	0.92	0.34	0.72
D	0.06	0.92	0.15	0.70
E	0.045	0.91	0.12	0.67
F	0.03	0.90	0.08	0.64
“G”	0.02	0.89	0.05	0.61

Appendix C. Stability-dependent power-law wind profiles

The puff meander code has an option for using a power-law wind profile for extrapolating between the wind measurement height and the puff release height. This option is useful, for example, if the wind measurements are near the surface and the release is well above the surface. For this case, the puff may travel too slow if the near-surface wind measurements are used. The power-law profile option extrapolates the wind speed from the measurement height to the release height based on commonly observed stability-dependent wind profiles in the surface layer (e.g., see Arya, 1988). Although these approximations have been found to hold true on average, any one case may be significantly different. Complex terrain conditions can further degrade the power-law wind profile assumption. Below, we give the form of the power-law wind profile corrections found in the puff meander code and the following page shows typical power-law profiles plotted as a function of stability.

Equation C1. Power-law wind profile formula.

$$\overline{U} = \overline{U}(z_m) \cdot \left(\frac{z}{z_m}\right)^p$$

where z_m is the measurement height and p is the stability dependent power-law exponent.

Table 1: Power-Law Wind Profile Exponent

exponent p	stability class
0.07	A-B
0.10	C
0.15	D
0.35	E
0.55	F

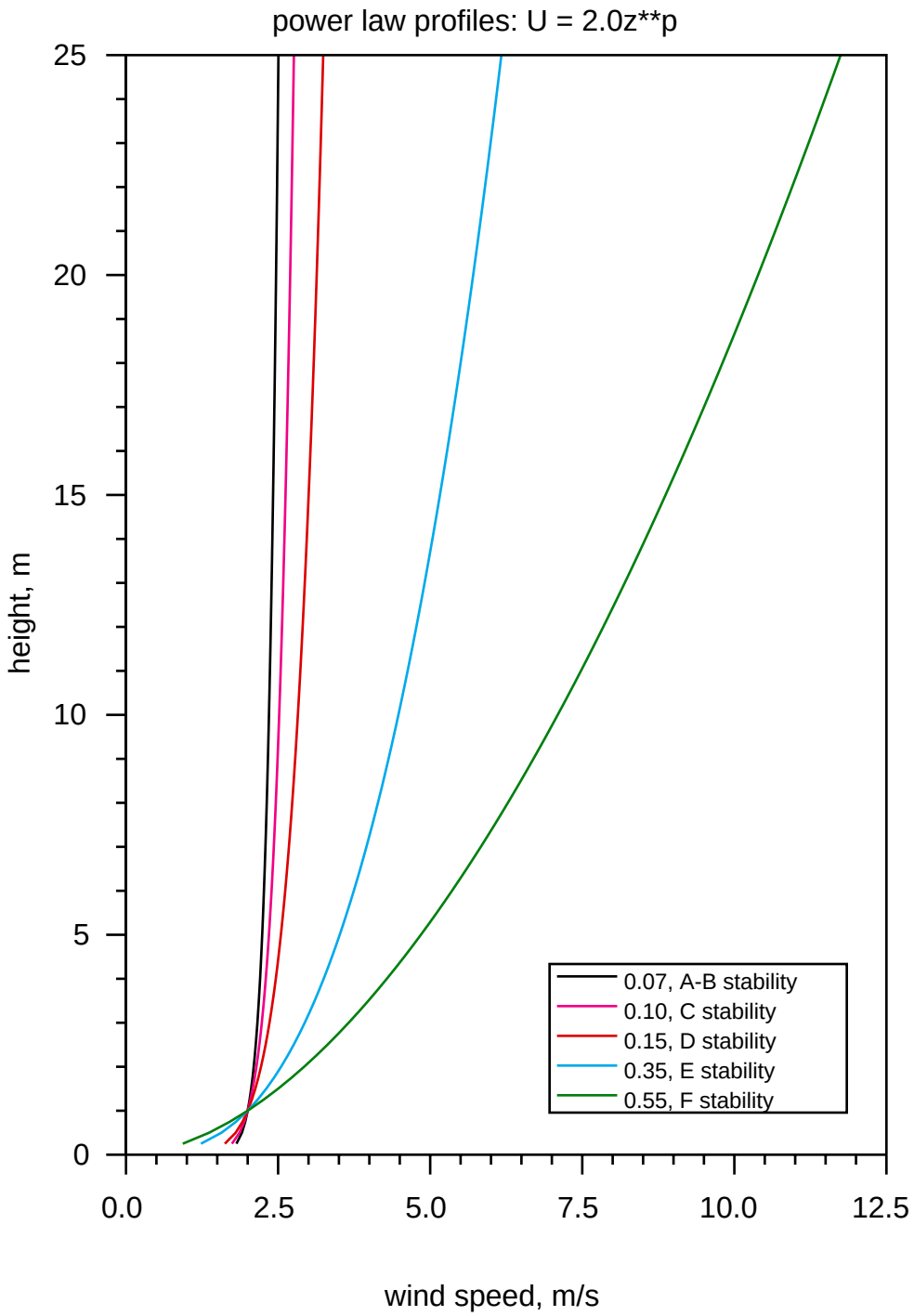

Figure C1. Power-law wind profiles given by Eqn. C1 for different stability classes using z_m = 1 m and $U(z_m)$ = 2.0 m/s.